JOURNAL OF AIRCRAFT
Vol. 37, No. 6, November–December 2000

Viscous Compressible Flow Across a Hole in a Plate

George R. Inger*
Iowa State University, Ames, Iowa 50011-3231
and
Holger Babinsky†
University of Cambridge, Cambridge, England CB2 1PZ, United Kingdom

Many aerodynamic flow control devices make use of wall transpiration as a means of influencing boundary-layer behavior. The use of drilled-hole plates has come to be preferred for this purpose. To evaluate the aerodynamic performance of such plates in either a real physical system or its computational-fluid-dynamics modeled simulation, it is crucial to have an accurate knowledge of how the mass flow through the plate hole depends on the driving pressure difference across the plate as a function of the relevant parameters such as hole diameter, plate thickness, and the properties of the gas. This paper offers a new unified theoretical model of viscous compressible flow across a hole, which gives the designer or numerical analyst of transpiration systems the ability to conveniently predict the characteristics of a porous plate a priori for any given flow conditions. Validating comparisons with experimental data are also presented.

Nomenclature

A	= hole cross-sectional area ($\pi D^2/4$)
$C_{1,2,3,4}$	= various constants in theory; Eqs. (1–3)
C_m	= $(\dot{m}/p_1 A)\sqrt{(\gamma RT)}$; Eq. (14)
C_μ	= constant defined following Eq. (14)
D	= effective circular diameter of hole
l_i	= entry length; Fig. 1
M	= local Mach number $[V/\sqrt{(\gamma RT)}]$
$\dot{m}$	= mass-flow rate
p	= static pressure
p_0	= total (stagnation) pressure
R	= ideal-gas constant ($p = \rho RT$)
Re_{EFF}	= effective Reynolds number of hole flow; Eq. (8)
T	= absolute static temperature
t	= plate thickness
V	= cross sectionally averaged flow velocity
$\mathcal{V}$	= nondimensionalized velocity $[V/\sqrt{(RT)}]$
x	= streamwise coordinate along hole
γ	= specific heat ratio
κ	= constant in Eq. (7)
μ	= coefficient of viscosity
ρ	= cross sectionally averaged density
τ_w	= local wall skin friction; Fig. 2

Subscripts

1	= hole entrance station; Figs. 1 and 4
2	= hole exit station; Figs. 1 and 4

Introduction

MANY aerodynamic flow control devices make use of wall transpiration as a means of influencing boundary-layer behavior. Examples include the distributed suction gloves used in laminar flow control, localized blowing systems used in place of vortex generators, and passive control devices used to alleviate the effects of shock/boundary-layer interactions.[1] The critical element in such devices is the perforated wall structure itself. With the advent of computer-controlled laser or electron beam manufacturing techniques, the use of drilled-hole plates of either metal or composite metal has come to be preferred, thus avoiding the weight and strength problems associated with more conventional porous materials. Typical plates can thereby be quickly and cheaply drilled with holes as small as 50 μm in order to minimize excrescence drag; the desired porosity is then achieved by adjusting the hole spacing.

To evaluate the aerodynamic performance of such plates in either a real physical system or its computational fluid dynamics (CFD)-modeled simulation, it is crucial to have an accurate knowledge of how the mass flow through the plate hole depends on the driving pressure difference across the plate as a function of the relevant parameters such as hole diameter, plate thickness, and the properties of the gas. Moreover, it has proven equally important in experimental and computational-simulation work that this mass-flow pressure relationship be 1) soundly based in fundamental physical principles and 2) expressed in an analytical form that is tractable for application. Although several theories of holed-plate behavior have been proposed so far, none have proved fully satisfactory in meeting these requirements: those that are analytically simple do not give an accurate account of the compressibility effects that arise in practical applications, whereas those which show agreement with experimental measurements are either awkward to use in practice or are based on largely empirical models with unclear basic physics. The present paper offers a unified theoretical model of drilled-hole flow, which redresses these shortcomings and gives the designer or numerical analyst of transpiration systems the ability to predict conveniently the characteristics of a porous plate a priori for any given flow conditions.

We first give a brief review of previous work on the problem and an assessment of the various basic assumptions needed to capture the essential physics of the problem. Based on this, a fundamentally based theory of the hole flow is presented, which results in a closed-form relationship for the mass flow vs pressure ratio that includes compressibility effects. An important byproduct of this analysis is shown to be a new universal similitude law governing the flow for all hole-size/plate-thickness/gas-property combinations, which involves a single relevant characteristic Reynolds number of the problem based on at appropriate thermal reference velocity. This is followed by a discussion of how the hole flow theory is adapted to the exterior environment of practical applications. Finally, we present some validating comparisons with experimental data.

Presented as Paper 99-3191 at the 17th Applied Aerodynamics Conference, Norfolk, VA, 28 June–1 July 1999; received 20 July 1999; revision received 11 August 2000; accepted for publication 18 September 2000.

*Professor, Department of Aerospace Engineering and Engineering Mechanics. Associate Fellow AIAA.
†Lecturer, Department of Engineering. Member AIAA.

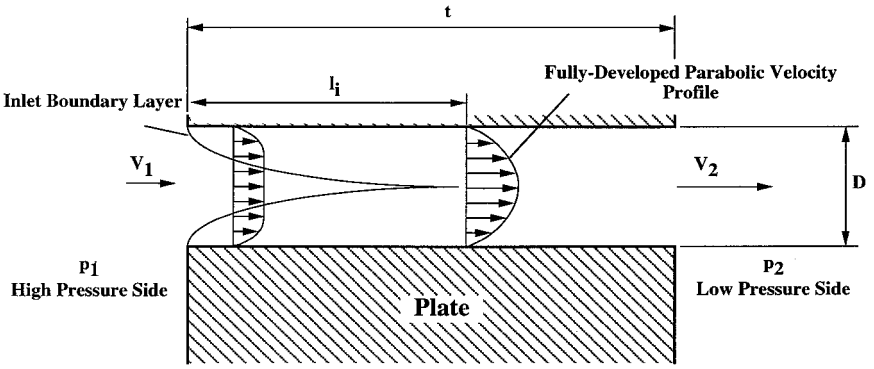

Fig. 1 Schematic of hole flow including entry region.

Brief Review of Previous Theoretical Work

We consider steady flow of an ideal gas through constant-area holes drilled in a uniform plate, caused by an imposed pressure difference across the plate (Fig. 1). Over the range of operating conditions encountered in practical transpiration systems,[2] it has been agreed that the required hole size and spacing is such that interhole interference is negligible, i.e., each hole behaves in isolation from the rest. Moreover, the corresponding hole Reynolds numbers based on the expected mass flows are always so low (50–100 or less) that the flow within the hole may be taken as laminar and "pipe like." However, the anticipated plate-thickness-to-hole-diameter ratios in practice are often not large enough to regard the flow as fully established throughout, so that inlet effects must be taken into account. Finally, in many passive transpiration control systems currently under study the pressure differences needed to produce the requisite mass-flow rates imply accelerations across the hole, which make compressibility an important factor in the analysis.

We now assess existing theoretical work in the light of these requirements. The simplest conceivable model would be to assume a direct proportionality of the hole flow exit velocity V_2 (mass flow) to the overall driving pressure difference Δp in the form suggested by the Poisseiuille solution for fully developed slow flow in a pipe.[3] Such an approach, termed a modified D'Arcys Law, has in fact been proposed in the form

$$V_2 = C_1(D^2\Delta p/32\mu t) \tag{1}$$

where C_1 would be taken as unity if the flow were truly developed and incompressible throughout the hole. In practice, this relationship has been found to be applicable only for very small Δp and then only when C_1 is assigned a nonunity empirical value that depends on the flow and is chosen to fit experimental data. Thus, although simple in form Eq. (1) is insufficient to capture the combined compressibility and inlet flow development effects that are important in practice.

Instead of such a viscous-dominated flow model, other investigators (e.g., Ref. 4) have gone to the opposite extreme by proposing a purely inviscid model entailing isentropic nozzle flow. Such an approach yields the expression

$$V_2 = (\gamma RT_2)^{\frac{1}{2}} C_2 \sqrt{[2/(\gamma-1)]\left[(p_1/p_2)^{(\gamma-1)/\gamma} - 1\right]} \tag{2}$$

where the nonunity constant C_2 is again an empirically chosen value that depends on Reynolds number and D/t ratio according to a suitable data fit. An even less fundamentally based variant of this model has been proposed[5] in which the product C_2 times the square root in Eq. (2) is replaced by the entirely empirical expression $1.2(\Delta p/p_2)^{0.55}$. In either case the resulting theory obviously does not capture the basic physics of either the compressibility or viscous effects residing in the mass and momentum conservation of the flow.

Yet another model that has been proven popular in contemporary transpiration system studies is the one proposed by Poll et al.,[2] who developed a relationship between V_2 and Δp on the basis of assumed incompressible pipe flow that takes the quadratic form

$$Y = C_3X + C_4X^2 \tag{3}$$

where $Y \equiv \rho D^4\Delta p/\mu^2t^2$ and $X = \pi D^2V^2/\mu t$ are nondimensional variables obviously influenced by the form of D'Arcy's law and C_3, C_4 are constants. Although solution of Eq. (3) for V_2 obviously provides a simple $V_2 - \Delta p$ relationship, the constants C_3 and C_4 yet again must be chosen empirically to make the equation work in practice with the resulting values of C_3 and C_4 proving dependent on both Reynolds and Mach numbers. We conclude that there is still important physics missing from model Eq. (3).

Unlike the aforementioned theoretical models, which all contain insufficient flow physics and hence empirically-chosen "constants," Gibson[6] has recently offered a treatment that embraces both frictional and compressibility effects, along with an account of the inlet influence that avoids the need to assume fully developed flow in the hole. His approach employs classical Fanno analysis for an adiabatic one-dimensional constant-area pipe flow[7] combined with Langhaar's treatment of the entry length effect on the skin friction.[8] The resulting predictions involve only a single universal numerical constant and show good agreement with mass flow vs Δp calibration data over a wide range of Δp and plate flow conditions. Unfortunately, this success is tempered by significant practical drawbacks: the method, although sound, is tedious and does not provide an explicit relationship between V_2 and Δp. Its use in practice thus requires an interactive procedure that proves awkward and expensive to use in design or computer simulation code work. Nevertheless, one draws from Gibson's work the inspiration that perhaps a more tractable, yet still fundamentally based, approach might be possible.

Proposed New Theory for Flow Inside the Hole

Analysis

The foregoing assessment suggests that a suitably comprehensive yet analytically tractable new theory of the hole flow problem, free from empirical constants, would be of value. With reference to the flow schematic illustration in Fig. 1, we adopt a quasi-one-dimensional flow model involving the average flow properties of density ρ and velocity V across each local area cross section along the direction x of flow; for constant area $A = \rho D^2/4$ this is governed by the continuity equation

$$\rho V = \text{const} = \rho_1V_1 = \rho_2V_2 \tag{4}$$

Allowing in the general case for inertial effects, consideration of the momentum balance for any elemental disk of the flow (Fig. 2) would further require that

$$\rho AV\,\mathrm{d}V = -A\,\mathrm{d}p - \pi D\tau_w\,\mathrm{d}x \tag{5}$$

where τ_w is the local (laminar) wall skin friction. When supplemented by the ideal-gas equation of state

$$p = \rho RT \tag{6}$$

and an account of the energy aspect of the problem (to determine T), Eqs. (4) and (5) contain all of the essential physics of the problem once an appropriate model for τ_w is introduced that includes the entry

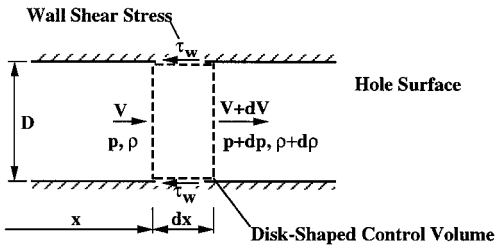

Fig. 2 Typical disk element of hole flow.

effect wherein the side-wall boundary layer grows and engulfs the uniform inlet flow V (Fig. 1).

We now introduce such a τ_w model under the basic assumption that each local disk of flow behaves like a slice of non-fully developed pipe flow taken at the prevailing local density and velocity. Restricting attention to hole lengths t that are greater than the entry length l_i (which embraces the vast majority of practical cases), this model yields the following expression upon inclusion of Langhaar's entry length effect correction[8]:

$$\tau_w = (8\mu V/D)[1 + (\kappa - 1)(D/t)(l_i/D)] \tag{7}$$

where both the entry length ratio $l_i/D \approx 0.057/(\rho_1 V_1 D/\mu)$ and the universal constant κ are given from first principles by the detailed pipe inlet analysis of Schlichting.[3] Gibson[6] has suggested that a value of κ in the range 2.5–3 fits a wide range of practical cases. The other element of our proposed theory, which completes the physical model, is the assumption that the gas temperature and hence the coefficient of viscosity varies only slightly across the plate so that the flow can be taken as isothermal at some suitable value (e.g., the average temperature of the plate). This is justified by the fact that the biggest temperature change occurs between Mach numbers of 0 and 1, when the flow accelerates from rest (i.e., outside the hole). Because the flow Mach number on entry and exit is likely to be of a similar order of magnitude, the change of temperature calculated from an adiabatic assumption is quite small. It is unlikely that the flow through the holes is adiabatic; hence, the isothermal assumption is not unrealistic. Isentropic flow calculations (an alternative but more complicated assumption) show that the static temperature variations along the flow are indeed rather small up to choked flow conditions. As a result of this simplification, the local density varies directly with the pressure along the flow by virtue of Eq. (6).

The foregoing physical model contains the combined effects of viscous friction (including the influence of entry length) and compressibility for any ideal gas. Even more remarkably, it is capable of a closed-form solution for the exit velocity as a function of the driving pressure ratio p_1/p_2. Thus with T and hence μ as known constants, substitution of Eqs. (4), (6), and (7) into the momentum equation (5) followed by some algebraic rearrangement yields the pressure-governing differential equation

$$\frac{p\,\mathrm{d}p}{p_2^2} - \left(\frac{V_2}{\sqrt{\gamma RT}}\right)^2 \frac{\mathrm{d}p}{p} = -\frac{\left(V_2|\sqrt{RT}\right)}{Re_{\mathrm{EFF}}}\,\mathrm{d}\left(\frac{x}{t}\right) \tag{8}$$

where

$$Re_{\mathrm{EFF}} = \frac{\rho_2 D\sqrt{RT}}{32\mu[1 + 0.057\kappa(D/t)(\rho_1 V_1 D/\mu)]t/D}$$

is a single master effective Reynolds number that contains the influence of the entry length effect. Now Eq. (8) can obviously be integrated term by term across the plate; however, before doing so inspection suggests that it would be convenient to regard $\sqrt{(RT)}$ as the appropriate thermal reference velocity of the problem, and hence introduce the nondimensional pressure and exit velocity variables p/p_2 and $\mathcal{V} \equiv V_2/\sqrt{(RT)}$, respectively. The resulting universal form of Eq. (8) can then be integrated from $p = p_1$ at $x = 0$ to $p = p_2$ at $x = t$ to give

$$\tfrac{1}{2}\left[(p_1/p_2)^2 - 1\right] - \mathcal{V}^2 \ln(p_1/p_2) = \mathcal{V} Re_{\mathrm{EFF}} \tag{9}$$

Tracing back to the original momentum equation, we note that the first term on the left derives from the pressure gradient effect, whereas the second term comes from the inertia effect associated with isothermal compressibility and the last term on the right, of course, derives from the viscous skin friction including the entry length effect. Equation (9) is seen to be a simple quadratic equation for the nondimensional exit velocity in terms of p_1/p_2; its solution excluding the negative root gives us the desired mass-flow vs pressure-ratio relationship

$$\mathcal{V} = \frac{\sqrt{1 + 2Re_{\mathrm{EFF}}^2\left[(p_1/p_2)^2 - 1\right]\ln(p_1/p_2) - 1}}{2Re_{\mathrm{EFF}}\ln(p_1/p_2)} \tag{10}$$

This equation enables the direct prediction of the mass flow pertaining to any given pressure ratio for any type of gas at any temperature flowing across holes of arbitrary t and D. It also provides a fundamentally based and simple analytical link between the conditions on the two sides of the plate that should prove useful in experimental design and in computational simulations of either active or passive transpiration systems for shock/boundary-layer interaction control.

The present analysis can be regarded as an extended version of the classical theory of isothermal laminar-frictional one-dimensional ideal-gas flow in a tube (e.g., Ref. 7) in which entry effects and a particularly advantageous closed-form solution for the mass-flow vs driving-pressure ratio have been added. Furthermore, an important new similitude property of the problem is included (see the following).

Similitude Properties

Some reflection about the nondimensional form of both Eqs. (9) and (10) shows that the present theory embodies an interesting and useful new similitude property of all hole flows: the nondimensional exit velocity $\mathcal{V}$ (which in fact equals $\sqrt{\gamma}$ times the exit flow Mach number) is a function only of the driving pressure ratio and the single master reference Reynolds number just defined. Thus, as illustrated in Fig. 3, a plot of $\mathcal{V}$ vs p_1/p_2 according to Eq. (10) will yield

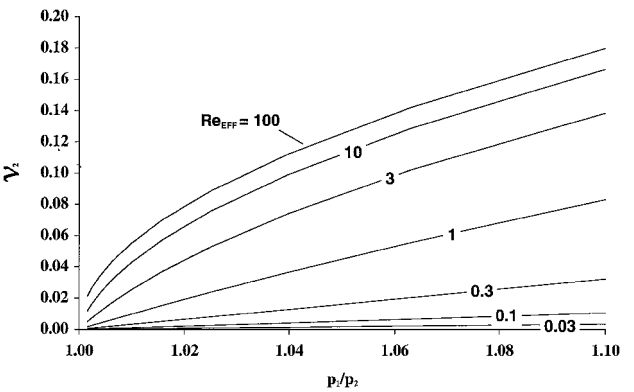

a) Small pressure differences

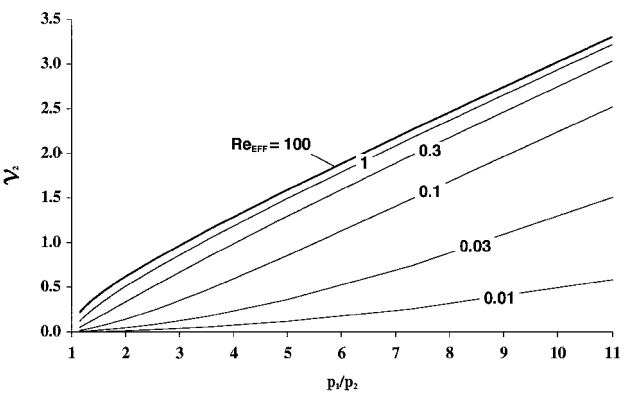

b) Medium-to-large pressure differences

Fig. 3 Master plot of nondimensional exit velocity vs pressure ratio.

a unique family of curves with Re_{EFF} as the single parameter. In addition to thereby providing an efficient display of all possible solution regimes including the combined effects of viscosity, entry length, and compressibility, this similitude property can prove useful in experimental design and in the correlation of data taken at various different conditions.

Limiting Cases

A number of significant features can be discerned by closer examination of Eqs. (9) and (10) plus the associated plots shown in Fig. 3. First, it is seen from Fig. 3a that when the pressure difference $\Delta p/p_2$ is very small ($p_1/p_2 \rightarrow 1$) and Re_{EFF} of order unity or less, the mass flow is a linear function of $\Delta p/p_2$ with a slope directly proportional to Re_{EFF}. This result can be physically understood by analyzing the asymptotic behavior of Eq. (10) in the limit where $(\Delta p/p_2)Re_{EFF} \ll 1$; this yields

$$\mathcal{V} = (\Delta p/p_2)Re_{EFF} \tag{11}$$

which is in fact D'Arcy's law for slow viscous-dominated incompressible pipe law when reexpressed in the present similarity variables and extended to included the inlet flow development effect.

A second important feature can be perceived from inspection of Fig. 3b, which embraces a much wider range of pressure differences that are in general not small: here it is seen that for $Re_{EFF} \geq \mathcal{O}(1)$ the family of $\mathcal{V}$ vs p_1/p_2 curves above $\Delta p/p_2 \geq 0.03$ collapse into a single Reynolds-number-independent locus that is nearly linear (but with a nonzero intercept) at larger p_1/p_2. This inviscid behavior can be understood by again examining the asymptotic behavior of Eq. (10), but this time in the limit where $Re_{EFF}^2[(p_1/p_2)-1]$ is large; this yields

$$\mathcal{V} \cong \sqrt{\frac{(p_1/p_2)^2 - 1}{2\,\ell n(p_1/p_2)}} \tag{12}$$

which for $(p_1/p_2)^2 \gg 1$ becomes proportional to p_1/p_2 with a slight modulation by the slowly varying logarithmic factor. We further note that this limiting behavior has a rough resemblance to the semi-empirical isentropic nozzle flow model of Eq. (2), except, of course, that Eq. (12) further embraces full consideration of mass and momentum conservation.

A third point to note is that our quadratic Eq. (9) for $\mathcal{V}$ is similar in form to the semi-empirical relationship (3) of Poll et al.[2] except that it is a more general fundamentally based result that includes both the compressibility and inlet length aspects of the problem.

Application of the Theory in Practical Situations

Adaptation to the Environment Surrounding the Hole

For most practical applications the number and site of holes is small compared to the area of solid wall, i.e., the porosity is small (<10%). Hence we assume that the average pressure on the outer surface of the porous wall is equivalent to the total pressure p_0. In the case of the porous surface being underneath a boundary layer (i.e., suction on a wing), the air entering the holes is assumed to originate from the very bottom of the boundary layer, where it is at rest with a pressure equivalent to the average surface pressure. With reference to Fig. 4, the air entering a hole undergoes an isentropic acceleration from rest. The pressure at hole entry p_1 and the velocity at hole entry V_1 are related by isentropic relationships:

$$p_1/p_0 = \left\{1 + [(\gamma - 1)/2]M_1^2\right\}^{-\gamma/(\gamma-1)} \tag{13}$$

The air leaving on side 2 forms a jet, and the pressure at the surface is equivalent to the static pressure in the jet. In cases where the air enters into a cavity, the assumption is made that the cavity pressure is p_2. The eventual breakdown of the jet could theoretically increase the cavity pressure, but because the size of the cavity is likely to be much larger than the hole dimensions, the assumption is made that the losses associated with the shear layer lead to an eventual cavity pressure that is not significantly above the static pressure in the original jet. The pressure difference driving the flow through the porous surface is therefore $p_0 - p_2$. Although seldom appreciated, the pressure p_1 that is often measured or used in CFD simulations is in fact the upstream total pressure p_0 rather than the upstream static pressure p_1.

Choking Behavior

The foregoing solution exhibits a maximum in the mass-flow rate vs pressure-ratio variation that becomes apparent when Eq. (9) is rewritten in terms of the nondimensional mass-flow parameter $C_m \equiv [\dot{m}/(p_1 A)]\sqrt{(RT)}$. Substituting the resulting value $\mathcal{V} = (p_1/p_2)C_m$ into Eq. (9) thus yields the following quadratic relationship governing C_m:

$$C_\mu C_m = \tfrac{1}{2}\left[1 - (p_2/p_1)^2\right] + C_m^2\,\ell n(p_2/p_1) \tag{14}$$

where the const $C_\mu \equiv 32[1 + 0.57\kappa(D/t)\rho_1 V_1 D/\mu]\mu RT/Dp_1$. As illustrated in Fig. 5, Eq. (14) predicts a maximum in C_m vs p_1/p_2, which differentiation with respect to p_2/p_1 shows will occur when $C_m = C_{m,MAX} = p_2/p_1$, corresponding to the slightly subsonic exit Mach number value of $M_2 = \gamma^{-1/2}$ (which pertains to an isothermal Mach number of unity). With further increase in the pressure ratio above that for $C_{m,MAX}$, the mass flow slowly decreases, asymptotically approaching the curve $C_m \sim (\ell n\, p_1/p_2)^{-1/2}$ at large pressure ratios as shown in Fig. 5.

To see such choking behavior in a practical calculation, one must hold the total pressure p_0 on the supply side constant while lowering

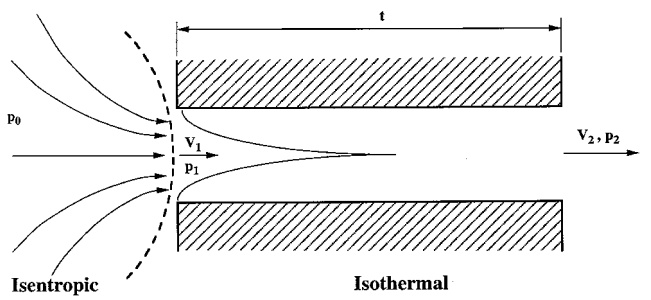

Fig. 4 Practical application of the analysis.

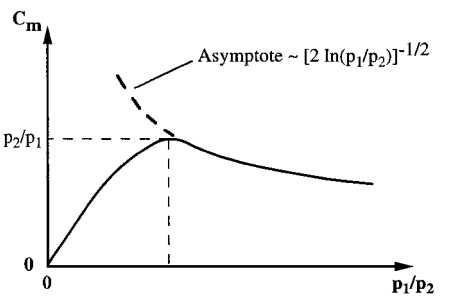

Qualitative trend

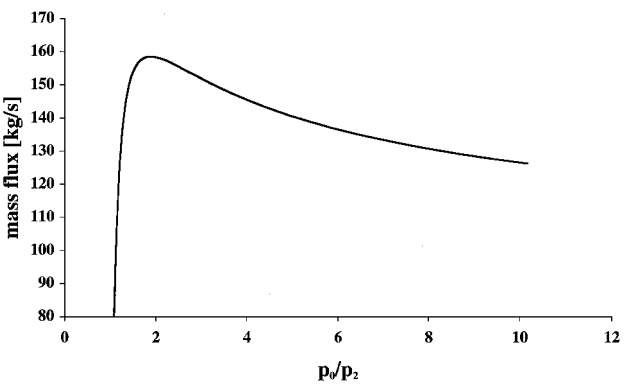

Sample practical calculation

Fig. 5 Mass-flow vs pressure-ratio behavior.

the exit pressure p_2; alternatively varying p_0 while holding p_2 fixed merely serves to increase the entering air density more and more with a consequent monotone increase in the mass-flow rate.

Experimental Validation

To assess the accuracy of the proposed theory, mass-flow vs pressure-difference measurements were carried out at Cambridge University using porous plate samples placed in a pressurized duct (Fig. 6). The laser-drilled holed plates used were supplied by the British Aerospace Sowerby Research Center and made of 0.91-mm-thick duraluminum; the holes were 75 μm in diameter (nominal) and distributed uniformly over the plate face with different degrees of porosity (2 and 4%). Operating with air at standard room temperature, various levels of pressurization p_1 were imposed to drive the flow across the porous plate into the lower pressure region downstream. The actual resulting mass flow was then measured yet farther downstream by a standard orifice plate flow meter arrangement as indicated in Fig. 6.

All pressures were measured using manometers with an accuracy of better than 0.5%. Taking this error as well as other uncertainties into account , the measurement of mass flux using the orifice plate configuration seen in Fig. 6 is accurate to within $\pm 1\%$. However, the actual magnitude of plate porosity is a major source of uncertainty. Although the plates were manufactured to a high standard, it is uncertain what the exact open-to-closed area ratio is. Furthermore it was often found that individual holes were blocked with dirt, which, in extreme cases, reduced the effective open-to-closed area ratio by almost 20%. The results presented here were obtained on carefully cleaned plates; however, the variation in the actual value of the open area of a given plate remains the largest source of uncertainty. Because the data shown in Fig. 7 are nondimensionalised by the total hole area, the values of $\dot{m}/A$ are affected by this uncertainty, which is estimated to be of the order of $\pm 10\%$. Some representative error bars are included in Fig. 7.

An example of the calibration curve so obtained is shown in Fig. 7 for two plates each of 2 and 4% porosity (typical values of interest in transpiration system applications), where the mass flow per open area produced by various driving pressure differences $\Delta p = p_0 - p_2$ is plotted. The data are seen to follow the expected trend of $\dot{m}/A$ increasing monotonically but nonlinearly with Δp. Also indicated on Fig. 7 is the corresponding curve obtained from Eq. (10) for the same operating conditions, from which it can be seen

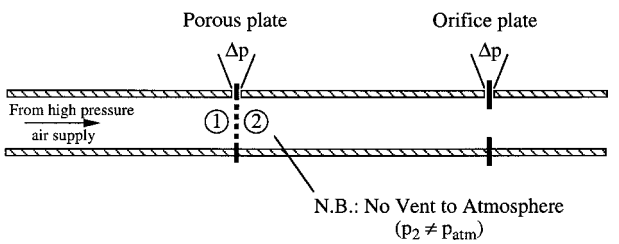

Fig. 6 Apparatus used to determine porous plate mass-flow calibration curve.

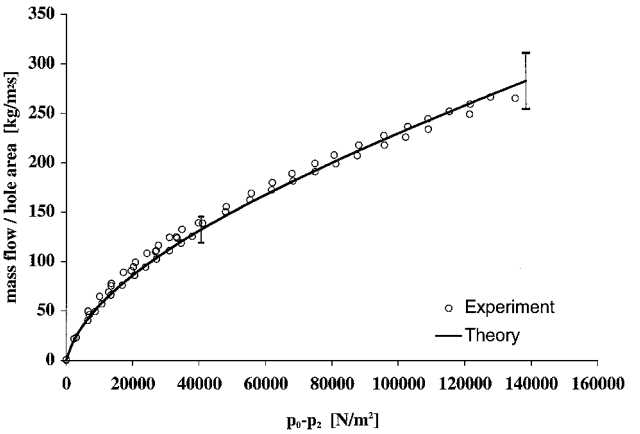

Fig. 7 Comparison of present theory with experiment.

that the theory accurately predicts both the magnitude and shape of the experimental curve over the rather wide range of Δp considered.

Concluding Remarks

This paper has presented a new unified theoretical model of viscous compressible flow across a hole which gives the designer or numerical analyst of transpiration systems the ability to conveniently predict the characteristics of a porous plate a priori for any given flow conditions. Validating comparisons with experimental data were also presented. In future work other such comparisons will be presented at different porosities as well as new data plus theory dealing with the effect of plate hole diameter.

References

[1] Atkin, C. J., and Squire, L. C., "A Study of the Interaction of a Normal Shock Wave with a Turbulent Boundary Layer at Mach Numbers Between 1.30 and 1.55," *European Journal of Mechanics B/Fluids*, Vol. 11, No. 1, 1992, pp. 93–118.

[2] Poll, D. I. A., Danks, M., and Humphries, B. E., "The Aerodynamic Performance of Laser Drilled Sheets," *Proceedings of the First European Forum on Laminar Flow Technology*, DGLR Rept. 92-06, Bonn, 1992, pp. 274–277.

[3] Schlichting, H., *Boundary Layer Theory*, 7th ed., McGraw–Hill, New York, 1979, pp. 185, 186.

[4] Abrahamson, K. W., and Brewer, D. L., "An Empirical Boundary Condition for Numerical Simulation of Porous Plate Bleed Flows," AIAA Paper-88-0306, Jan. 1988.

[5] Bohning, R., and Doerffer, P., "Passive Control of Shock Wave–Boundary Layer Interaction and Porous Plate Transpiration Flow," *Notes on Numerical Fluid Mechanics*, edited by E. Stanewsky, J. Déléry, J. Fulker, and W. Geißler, Vol. 56, Viewig, Brunswick, Germany, 1997.

[6] Gibson, T., "The Passive Control of Shock Wave/Boundary Layer Interactions," Ph.D. Dissertation, Engineering Dept., Cambridge Univ., Cambridge, England, U.K., 1997.

[7] Shapiro, A., *Dynamics and Thermodynamics of Compressible Flow*, Vol. 1, Roland Press, New York, 1953, Chap. 6, p. 189.

[8] Massey, B. S., *Mechanics of Fluids*, 6th ed., Chapman and Hall, London, 1989, pp. 448–455.